Model Calculations of Potential Surfaces of van der Waals Complexes Containing Large Aromatic Molecules

Mary Jo Ondrechen,[†§] Ziva Berkovitch-Yellin,[‡] and Joshua Jortner*[†]

Contribution from the Department of Chemistry, Tel Aviv University, Tel Aviv, Israel, and Department of Structural Chemistry, The Weizmann Institute of Science, Rehovot, Israel. Received December 23, 1980

Abstract: In this paper we report the results of model calculations of the nuclear potential surfaces of van der Waals complexes consisting of large aromatic molecules and rare-gas (R) atoms. These potentials were constructed as a superposition of pairwise atom–atom potentials, the R–carbon atom pair potentials being taken from heats of adsorption of rare-gas atoms on graphite, while the R–hydrogen atom pair potentials are estimated by using empirical combination rules. The binding energies of the tetracene (T) complexes TR_1 are 0.7 kcal mol^{-1} for Ne, 1.5 kcal mol^{-1} for Ar, 1.8 kcal mol^{-1} for Kr, and 2.2 kcal mol^{-1} for Xe, while the equilibrium distance between R and the molecular plane of tetracene is 3.0 Å for Ne, 3.45 Å for Ar, 3.5 Å for Kr, and 3.7 Å for Xe. Low-frequency, large-amplitude motion of the R atoms parallel to the molecular plane along the long molecular axis is predicted for TR_1 and TR_2 complexes. The potential for TR_1 along the long molecular axis has a symmetric double-well form, giving rise to a "tunneling-type" motion of the R atom. For the TR_2 complexes, the configuration with two R atoms located on the same side of the aromatic molecule is energetically favored over that with the two R atoms on opposite sides. No chemical isomers are expected to exist for the TR_1 and TR_2 complexes, while for TR_n complexes with $n \geq 3$ the possibility of the existence of two or more nearly isoenergetic isomers is indicated. The applications and implications of these data for the elucidation of some features of excited-state energetics and dynamics of such van der Waals complexes are considered.

van der Waals (vdW) molecules[1-6] are weakly bound molecular complexes held together by attractive (e.g., dispersive, electrostatic, charge transfer, hydrogen bonding) interactions between closed-shell atoms or molecules. The primary characteristics of vdW molecules[1-6] are their low (10–1000 cm^{-1}) dissociation energies, the large length of the vdW bond, and the retention of many of the individual properties of the molecular constituents within the vdW complex. During the last few years remarkable progress was achieved in the understanding of the many facets of these interesting systems. These advances were initiated by the utilization of supersonic free expansions[3,4] to prepare a variety of fascinating vdW molecules, whose structure, energetics, and dynamics were explored. The elucidation of the structure, the mapping of the potential surface, and the determination of the energetics of vdW molecules pertain to the basic understanding of intermolecular interactions in chemistry. In this context the ground-state properties of a variety of molecules, e.g., $(HF)_2$,[7] ArHF,[8] ArHCl,[9] ArHBr,[10] KrHCl,[11] XeHCl,[12] ArClF,[13] ArOCS,[14] and the benzene dimer[3] were investigated. Studies of intramolecular dynamics of vdW molecules in vibrationally excited or electronically vibrationally excited states provided central information on reactive vibrational predissocation processes,[5-7] this being relevant for establishing the general features of intramolecular vibrational energy flow in weakly coupled molecular systems. Intramolecular dynamical processes in a variety of vdW molecules, e.g., RI$_2$ (R = He, Ne, and Ar),[15-17] $(Cl_2)_2$,[18] $(N_2O)_2$,[19] $(NH_3)_2$,[20] and the ethylene dimer[21] were recently explored both experimentally[15-21] and theoretically.[6] The understanding of the reactive and nonreactive dynamics in vdW complexes requires detailed information on potential surfaces. The general conceptual framework advanced for the elucidation of the structural and energetic features of all these small and medium-sized vdW complexes mentioned above rests on a microscopic approach, taking advantage of the advanced techniques of molecular spectroscopy[3-5,7-17] to probe the molecular equilibrium configuration, the details of nuclear motion, and the binding energies. This general approach may require some gross modifications when structure, energies, and dynamics of very large vdW complexes will be considered. Recently, there have been experimental studies[22-24] of very large vdW complexes consisting of aromatic molecules, such as anthracene, tetracene, pentacene, and ovalene

with rare-gas atoms. These vdW complexes were synthesized[22-24] in supersonic expansions of rare gas seeded with the aromatic molecules. Spectroscopic diagnostic methods were advanced[22-24] for the identification and characterization of the chemical composition of aromatic molecule–(rare gas)$_n$ complexes characterized by different coordination numbers n. The formation kinetics, excited-state energetics, electronic relaxation, and intramolecular vibrational dynamics were experimentally explored.[22-24] These studies are of considerable intrinsic interest as a very large vdW complex consisting of a large aromatic molecule and rare-gas

(1) Ewing, G. E. *Acc. Chem. Res.* **1975**, *8*, 185.
(2) Ewing, G. E. *Can. J. Phys.* **1976**, *57*, 487.
(3) Klemperer, W. *Ber. Bunsenges. Phys. Chem.* **1974**, *78*, 128.
(4) Smalley, R. E.; Wharton, L.; Levy, D. H. *Acc. Chem. Res.* **1977**, *10*, 139.
(5) Levy, D. H. In "Advances in Chemical Physics"; Jortner, J., Levine, R. D., Rice, S. A., Eds.; Wiley-Interscience: New York, 1981; Vol. 47, p 323.
(6) Beswick, J. A.; Jortner, J. "Advances in Chemical Physics"; Jortner, J., Levine, R. D.; Rice, S. A., Eds.; Wiley-Interscience: New York, 1981; Vol. 47, p 363.
(7) Dyke, T. R.; Howard, B. J.; Klemperer, W. *J. Chem. Phys.* **1972**, *56*, 2442.
(8) Harris, S. J.; Novick, S. E.; Klemperer, W. *J. Chem. Phys.* **1974**, *60*, 3208.
(9) Novick, S. E.; Davis, P. B.; Harris, S. J.; Klemperer, W. *J. Chem. Phys.* **1973**, *59*, 2273.
(10) Jackson, K. C.; Langridge-Smith, P. R. R.; Howard, B. J. *Mol. Phys.* **1980**, *39*, 817.
(11) Barton, A. E.; Henderson, T. J.; Langridge-Smith, P. R. R.; Howard, B. J. *Chem. Phys.* **1980**, *45*, 429.
(12) Chance, K. V.; Bowen, K. H.; Winn, J. S.; Klemperer, W. *J. Chem. Phys.* **1979**, *70*, 5157.
(13) Harris, S. J.; Novick, S. E.; Klemperer, W.; Falconer, W. E. *J. Chem. Phys.* **1974**, *61*, 193.
(14) Harris, S. J.; Janda, K. C.; Novick, S. E.; Klemperer, W. *J. Chem. Phys.* **1975**, *63*, 881.
(15) Smalley, R. E.; Levy, D. H.; Wharton, L. *J. Chem. Phys.* **1976**, *64*, 3266.
(16) Kim, M. S.; Smalley, R. E.; Wharton, L.; Levy, D. H. *J. Chem. Phys.* **1976**, *65*, 1216.
(17) Johnson, K. E.; Wharton, L.; Levy, D. H. *J. Chem. Phys.* **1978**, *69*, 2719.
(18) Dixon, D. A.; Herschbach, D. R. *Ber. Bunsenges. Phys. Chem.* **1977**, *81*, 145.
(19) Gough, T. E.; Miller, R. E.; Scholes, G. E. *J. Chem. Phys.* **1978**, *69*, 1588.
(20) Schutz, R.; Sudb, A. S.; Lee, Y. T.; Yen, Y. R. International Quantum Electronics Conference, Atlanta, GA, 1978.
(21) Hoffbauer, M. A.; Gentry, W. R.; Giese, C. F. *Springer Ser. Chem. Phys.* **1978**, *6*, xxxx.
(22) Amirav, A.; Even, U.; Jortner, J. *Chem. Phys. Lett.* **1979**, *67*, 9.
(23) Amirav, A.; Even, U.; Jortner, J. *J. Chem. Phys.* **1981**, *74*, 3745.
(24) Amirav, A.; Even, U.; Jortner, J. *J. Chem. Phys.* **1981**, *75*, 2489.

[†] Department of Chemistry, Tel-Aviv University.
[‡] Department of Structural Chemistry, The Weizmann Institute of Science.
[§] Department of Chemistry, Northeastern University, Boston, MA 02115.

atoms can be viewed as the aromatic "guest" molecule embedded in a well-defined local solvent configuration, whereupon solvent perturbations on excited-state energetics and dynamics can be explored from the microscopic point of view. At present there is no information available on ground-state structure on energetics of very large vdW complexes, such as aromatic molecule–(rare-gas)$_n$ molecules. Such information would provide the essential input data for the understanding of excited-state energetics and dynamics. The beautiful spectroscopic electric resonance and magnetic resonance techniques,[3,7-14] which led to a wealth of structural information concerning small and medium-sized vdW complexes, are not readily applicable to very large complexes. One approach toward the elucidation of ground-state structure and energetics of very large vdW molecules rests on model calculations of the intermolecular interactions. In this paper we report the results of such model calculations of the potential nuclear surface of vdW molecules, consisting of aromatic molecules and rare-gas atoms. As the most extensive experimental information[22,24] pertains to vdW complexes consisting of tetracene (T) and rare-gas (R) atoms, these TR$_n$ molecules were chosen as suitable candidates for our model calculations. The interaction potential between the rare-gas atoms and the very large aromatic molecule was constructed from a superposition of atom–atom pair potentials, while the interaction potential between rare-gas atoms was taken in the traditional Lennard-Jones form. The model calculations of the potential surface information are expected to elucidate the following features of these large complexes in their electronic ground state: (1) binding energies of rare-gas atoms in TR$_n$ complexes; (2) equilibrium configurations of TR$_n$ complexes; (3) nature of low-frequency nuclear motion of rare-gas atoms in TR$_n$ complexes; (4) exploration of the possibility of the existence of several nearly isoenergetic TR$_n$ chemical isomers characterized by a fixed value of the coordination number n, but with geometrically inequivalent sites for the R atoms.

Model Calculations

The potential energy for the nuclear motion of rare-gas atoms in a TR$_n$ complex was modeled on the basis of the following assumptions: (1) The high-frequency intramolecular nuclear motion within the aromatic molecule was frozen. (2) T–R and R–R pair interactions were considered. (3) The T–R interactions were represented in terms of atom–atom interactions between each C and H atom in the aromatic molecule and the rare-gas atoms. (4) The atom–atom interaction potentials exerted by the C atoms of the aromatic molecule upon the rare-gas atoms were expressed in the 6–12 form taken from the data of Crowell and Steele,[25] which faithfully reproduce the heats of adsorption of rare gases on graphite. The atom–atom interaction potential between a rare-gas atom and an H atom in the aromatic molecule were evaluated by using the well-known[26] empirical combination rules. (5) The R–R interaction pair potentials between rare-gas atoms were taken in the conventional 6–12 form. The potential energy $V(\{r_{I\alpha}\}, \{r_{IJ}\})$ for the motion of R atoms, located at the positions $\vec{r}_I$ (or $\vec{r}_J$), in the TR$_n$ complex is now determined by the distances $r_{I\alpha} = |\vec{r}_I - \vec{r}_\alpha|$ between each atom α in the aromatic molecule, which is located at $\vec{r}_\alpha$, and an R atom and by the distances $r_{IJ} = |\vec{r}_I - \vec{r}_J|$ between the rare-gas atoms. This potential energy is given by

$$V(\{r_{I\alpha}\}, \{r_{IJ}\}) = \sum_I V_{RA}(\{r_{I\alpha}\}) + \sum_I \sum_{<J} V_{RR}(r_{IJ}) \qquad (1)$$

Here, V_{RA} is the interaction potential between a single rare-gas atom and the aromatic molecule.

$$V_{RA}(\{r_{I\alpha}\}) = -\sum_\alpha A_{I\alpha}[r_{I\alpha}^{-6} - [(r_{I\alpha}^0)^6/2]r_{I\alpha}^{-12}] \qquad (2)$$

The parameters $A_{I\alpha}$ and $r_{I\alpha}^0$ for C–R interactions were taken from the work of Crowell-Steele,[25] and the H–R interactions were evaluated by using the combination rules[26]

$$A_{I\alpha} = (A_{II}A_{\alpha\alpha})^{1/2} \qquad r_{I\alpha}^0 = (r_{II}^0 + r_{\alpha\alpha}^0)/2 \qquad (3)$$

Table I. Potential Parameters for the Interaction of Rare-Gas Atoms with Aromatic Molecules[a]

α	I	$A_{I\alpha}$, kcal/mol	$r_{I\alpha}^0$, A
C	Ne	222	3.49
C	Ar	741	3.84
C	Kr	973	3.92
C	Xe	1570	4.14
H	Ne	168	3.24
H	Ar	560	3.60
H	Kr	734	3.68
H	Xe	1180	3.89

[a] Equations 3 and 4. Carbon–carbon R–R parameters taken from Crowell-Steele.[25] H–H obtained from Hirschfelder's values for H_2–H_2.[26]

Table II. Potential Parameters for Interaction between Rare-Gas Atoms[a]

R	A_{RR}, kcal/mol	r_{RR}^0, A
Ne	144	3.16
Ar	1597	3.87
Kr	2750	4.04
Xe	7140	4.46

[a] Taken from Crowell-Steele.[25]

with the C–R parameters taken from Crowell and Steele[25] and the H–H interactions adopted from the H_2–H_2 data given by Hirschfelder et al.[26] These potential parameters are presented in Table I. The potential V_{RR} in eq 1 represents the interaction between a pair of R atoms in the vdW complex being given by

$$V_{RR}(r_{IJ}) = -A_{RR}(r_{IJ}^{-6} - [(r_{RR}^0)^6/2] r_{IJ}^{-12}) \qquad (4)$$

The potential parameters are given in Table II. An alternative choice of atom–atom potential parameters for the interaction of the aromatic naphthalene molecule with Ar atoms was very recently proposed by Najbar and Turek.[27] At the present stage of embryonic development of the field we prefer our "semiempirical" potential parameters.

Finally, the geometry of the aromatic molecule has to be specified. In most of the present calculation the tetracene molecule was assumed to consist of four planar, regular hexagons with a carbon–carbon bond distance of 1.4 Å. Some calculations were conducted by using the actual planar geometry of the tetracene molecule using the C–C bond distances inferred from X-ray crystallography.[28] The C–H distances were taken to be 1.1 Å. In all calculations the perpendicular axis is designated z, the short axis x, and the long axis y.

The numerical data for the energetics of the TR$_n$ complexes will be presented within a chemical accuracy of 1 cal mol^{-1} (0.35 cm^{-1}) in order to facilitate a comparison with spectroscopic data,[22-24] which are accurate within 1 cm^{-1}. It should, however, be emphasized that our model calculations, which rest admittedly on crude potential, do not approach spectroscopic accuracy. Energy differences on a single potential surface, e.g., heights of potential barriers, are expected to be more accurate than energy differences between two potential surfaces, e.g., energies of two different complexes or two distinct isomers.

Results

TR$_1$ Complexes. For the interaction of tetracene with a single R atom (Ne, Ar, Kr, or Xe) the regions of minimum energy are 3–4 Å away from the molecular plane and are located over the centers of the inner rings. Table III shows the coordinates and minimum energies for the TNe$_1$, TAr$_1$, TKr$_1$, and TXe$_1$ complexes. We have tested the effects of the geometry of the tetracene molecule on the energetics and equilibrium configurations of the TR$_1$ complexes. The coordinates and energies of the TR$_1$ (R =

(25) Crowell, A. D.; Steele, R. B. *J. Chem. Phys.* **1961**, *34*, 1347.
(26) For example: Hirschfelder, J. O.; Curtiss, C. F.; Bird, R. B. "Molecular Theory of Gases and Liquids"; Wiley: New York, 1954; pp 168.

(27) Najbar, J.; Turak, A. M. *Chem. Phys. Lett.* **1980**, *73*, 536.
(28) (a) Robertson, J. M.; Sinclaire, V. C.; Trotter, J. *Acta Crystallogr.* **1961**, *14*, 697. (b) *Ibid.* **1962**, *15*, 289.
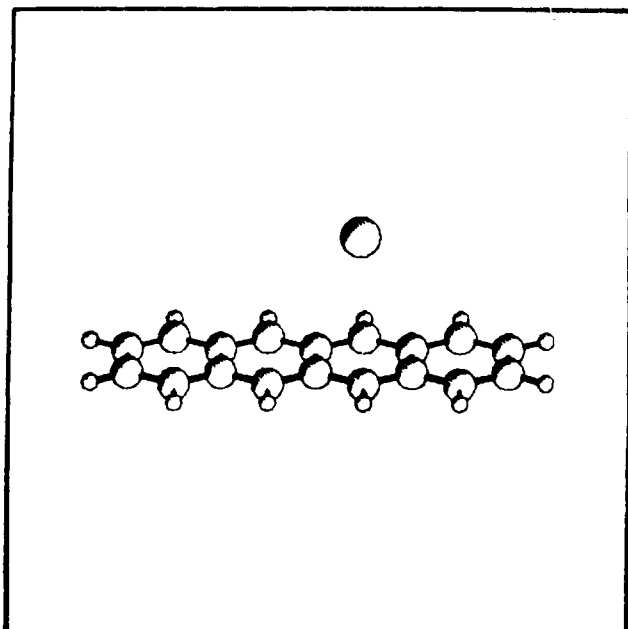
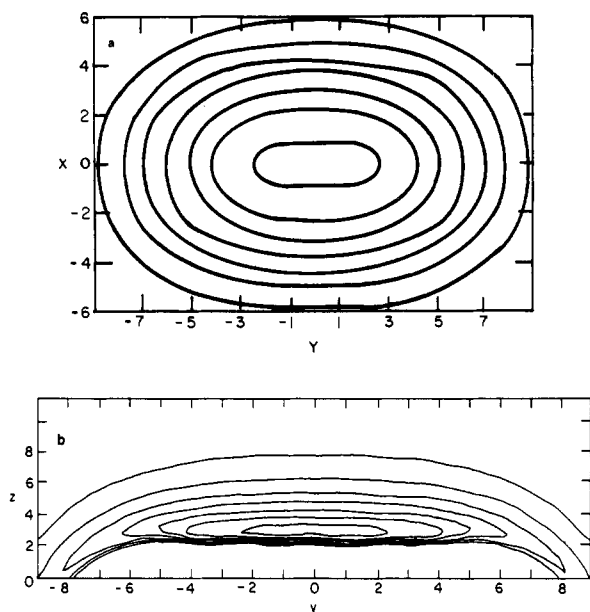**Figure 1.** Tetracene–Ar$_1$ in the minimum configuration.

Figure 2. Contour maps for the tetracene–Ar$_1$ potential for distance scales in Å. (a) Contour map in the plane z = 3.45 Å. The innermost contour is for B = −1.5 kcal mol^{-1} and subsequent contour intervals are 0.2 kcal mol^{-1}. Note that the tetracene molecule is located at 3.45 Å behind the section of the potential-energy surface as shown. (b) Contour map in the half-plane (x = 0; $z \geq$ 2.0 Å). Contour interval is 0.2 kcal mol^{-1}.

Ar, Kr, and Xe) complexes were calculated by using both the idealized geometry of tetracene, which was taken to consist of four benzene rings, and the actual geometry[28] of this molecule. As is apparent from Table III, the effects of the deviations of the C–C bond lengths from the idealized geometry on the binding energies of the R atom are negligibly small, being ~2 cm^{-1}. Similarly, the coordinates of minimum energy for the TR$_1$ complexes are found to be practically invariant (within the uncertainty of ±0.02 Å) to the change of the geometry of the tetracene molecule. We conclude that the effects of the deviations of the C–C bond lengths from the idealized geometry of the aromatic molecule are minor. Accordingly, all the subsequent calculations reported in this paper were conducted by utilizing the idealized geometry of the tetracene molecule.

Since tetracene has D_{2h} symmetry, there are four points of minimum energy in the potential surface for tetracene interacting

Table III. Potential Minima for Tetracene–R$_1$ Interaction

R	coordinates,[a,b] Å			energy, kcal/mol	
	x	y	z		
Ne	0.00	1.0	3.0	−0.71[b]	
Ar	0.00	1.10	3.45	−1.519[b]	−1.513[c]
Kr	0.00	1.10	3.50	−1.802[b]	−1.796[c]
Xe	0.00	1.00	3.70	−2.223[b]	−2.215[c]

[a] All coordinates are accurate to within ±0.05 Å, except for Ne, which is accurate to within ±0.02 Å. [b] Calculated using the idealized geometry of tetracene which was taken to consist of four benzene rings with all the C–C bond distances being 1.4 Å. [c] Calculated using the actual geometry of tetracene.[28]
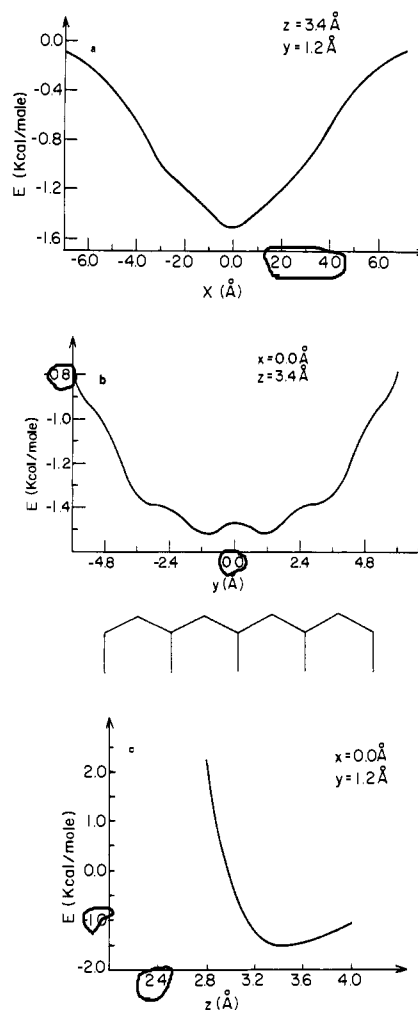

Figure 3. Interaction of tetracene with a single argon atom. (a) Potential energy (in kcal mol^{-1}) as a function of the x coordinate (in Å) along the line (y = 1.2, z = 3.4 Å). (b) Potential energy as a function of the y coordinate along the line (x = 0.0, z = 3.4). (c) Potential energy as a function of the z coordinate along the line (x = 0.0, y = 1.2).

with a single R atom. Figure 1 provides a view from the x axis of the TAr$_1$ complex, with the Ar atom located at one of these four minima. Figure 2a shows the potential in the xy plane at z = 3.45 Å, while Figure 2b shows sections in the half-plane defined by x = 0 and $z \geq$ 2.0. Details of the potential surface of TAr$_1$ are portrayed in Figure 3. Figure 3a presents the potential for motion in the x direction with a minimum at the center of the molecule. In Figure 3b the potential for the motion in the y direction is displayed, being symmetrical about the xz plane. The Ar atom sees two minima as it is moved along the long molecular y axis. Furthermore, these two minima are not located precisely over the centers of the two inner rings but are slightly displaced from the centers of the inner rings. The y coordinates of the geometric centers of the two inner rings are ±1.21 Å, while

the minima in the potential surface are located at $y = \pm 1.10$ Å. The symmetric double minimum potential along the y axis is of considerable interest. The most interesting issue concerns the location of the zero-point energy relative to the potential barrier which separates the two minima. The height of the potential barrier in TAr$_1$ is 0.05 kcal mol^{-1} (18 cm^{-1}). To estimate the zero-point energy, we have approximated the potential in the range $y = -2.4$–2.4 Å by the function[29]

$$V(Y) = A(Y^4 + BY^2) + AB^2/4 \qquad (5)$$

where $Y = A^{1/2}(2\mu/h^2)^{1/2}$, y represents the coordinate in dimensionless units, and μ is the mass of the Ar atom. The potential parameters A (cm^{-1}) and B (dimensionless) were determined from the positions of the minima $Y_{min} = \pm(|B|/2)^{1/2}$ and the barrier height $V_0 = AB^2/4$. Taking $Y_{min} = 1.1$ Å, together with $V_0 = 18$ cm^{-1}, results in $A = 1.4$ cm^{-1} and $B = -7.2$. Utilizing the numerical data[29] for the energy levels in the potential (5), the zero-point energy is estimated to be $E(0) = 5.0$ cm^{-1}. Accordingly, we expect that the zero-point energy for the motion of an Ar atom in the potential given in Figure 3b is located below the potential hump. The motion of the Ar atom in its ground state along the y axis bears a close analogy to the inversion motion of the ammonia molecule. The ground state of the system is expected to be symmetric with respect to reflection in the xz plane. However, at present we have just to draw two interesting but qualitative conclusions. First, we assert that the Ar atom motion along the long molecular axis is characterized by a large amplitude motion. Second, we note the appearance of a potential with two (or possibly more) minima. The potential barriers separating these minima originate from the effects of short-range repulsive interactions between the R atom and those carbon atoms which form C–C bonds parallel to the short molecular axis. The appearance of such multiple-humped potential will give rise to a tunneling-type motion of the R atoms in large vdW complexes of aromatics. Such effects will be characteristic of all linear aromatic polyacenes containing an even number of six-membered rings. A more detailed analysis of the nuclear dynamics will have to take into account the coupling between the nuclear motion along the y axis with the motion along the x and z axes, which will modify some of the quantitative details of the level structure.

Figure 3c shows the potential energy as a function of the z coordinate in the region of one of the minima. It bears a close resemblance to the familiar 6–12 form. Similar potential curves were obtained for the TKr$_1$ and TXe$_1$ molecules. From the potential in Figure 3c, and from similar plots for the TKr$_1$ and TXe$_1$ complexes, the frequency of vibrational motion perpendicular to the molecular plane may be estimated for the TR$_1$ complexes. To calculate this frequency, we assume that the potential curve along the z axis fits a Morse potential. The frequency ν is then given by

$$\nu = (6/r_0)(2D/\mu)^{1/2} \qquad (6)$$

where μ is the reduced mass and D is the dissociation energy uncorrected for zero-point motion. We take r_0 to be the z coordinate of the R atom at its minimum energy position, and D is the energy of the minimum of the potential. Table IV shows the frequencies obtained and the approximate number of bound vibrational levels in this potential, which is given by $2D/\omega$. Note that as the mass of the R atom increases, the number of bound levels and the depth of the well will increase, while the frequency decreases.

From these calculations of the potential surfaces of the TR$_1$ complexes, the following conclusions emerge.

(1) The binding energies of an R atom to the tetracene molecule vary from 0.71 for Ne to 2.22 kcal mol^{-1} for Xe. The increase of the binding energy with the atomic weight of R reflects the enhancement of dispersion interactions. These estimates of the binding energy correspond to the energies of the minima of the

(29) Laane, J. *Appl. Spectrosc.* **1970**, *24*, 73.
(30) For example: Rapp, D. "Quantum Mechanics"; Holt, Rinehart and Winston: New York, 1971; pp 170–7.

Table IV. Estimates of Frequency (ν), Dissociation Energy (D), and Number of Bound Vibrational Levels ($\mathcal{H}$) for the Perpendicular Vibrational Motion of a Rare-Gas Atom in TR$_1$ Complexes

	Ar	Kr	Xe
ν, cm^{-1}	57	45	41
D, cm^{-1}	532	630	777
$\mathcal{H}$	18	28	38

potential surface and do not contain the necessary corrections for the zero-point energy. As the zero-point corrections for the out-of-plane vibrational motion along the z axis are small, e.g., 0.08 kcal mol^{-1} for TAr$_1$ and 0.06 kcal mol^{-1} for TXe$_1$, they were not incorporated in the estimates of the binding energy.

(2) To obtain an estimate for the dependence of the energy of a vdW bond between an R atom and an aromatic molecule on the size of the aromatic molecule, we have compared the binding energies of tetracene–Ar ($D_0 = 1.52$ kcal mol^{-1}) and benzene–Ar ($D_0 = 1.12$ kcal mol^{-1}). In the latter case the equilibrium configuration involves the Ar atom being located above the center of the aromatic ring. The binding energy of an R atom to a linear polyacene will increase with the number, N, of aromatic rings, reaching near saturation at large N. On the other hand, the length of the vdW bond is less sensitive to N, being 3.45 ± 0.05 Å for TAr$_1$ and 3.45 ± 0.05 Å for benzene Ar$_1$.

(3) The nuclear motion of the R atom in the TR$_1$ complexes is characterized by a large amplitude and low-frequency motion. The height of the potential barrier for the motion of the R atom in the double minimum symmetric potential along the y axis is 18 cm^{-1} for Ar, 19 cm^{-1} for Kr, and 13 cm^{-1} for Xe. The tunneling motion of the R atom in the double minimum potential along the y axis is expected to be characterized by a very small tunneling splitting. For the motion of the Ar atom we have calculated a splitting of ~0.1 cm^{-1} between the zero-point energy and the first nuclear excited state. On the other hand, the vibrational frequency for the motion along the z axis is much larger.

(4) Only a single nuclear configuration of TR$_1$ complexes is expected to be energetically stable and no chemical isomers will be exhibited.

TR$_2$ Complexes. Without alluding to any numerical calculations one could argue that the binding of two R atoms to a large aromatic molecule will result in an energetically favored configuration with the two R atoms being located on the same side of the aromatic ring, this one-sided structure being stabilized by the attractive interaction between the pair of the R atoms. This expectation is borne out by our model calculations; however, not the entire R–R attractive interaction can be exploited for the stabilization of the TR$_2$ complex, in view of geometrical reorganization effects. Our model calculations for TAr$_2$, TKr$_2$, and TXe$_2$ demonstrate that with the first R atom being frozen in its minimum energy configuration a second R atom is unable to sit at the geometrically equivalent second site over the center of the unoccupied inner ring on the same face of the molecule. In such a configuration the R–R distance would be too short and the R–R repulsion would be too strong. However, the second R atom can sit at a point further away in the y direction corresponding to the optimum R–R distance. Even with the first R atom frozen at its original position of minimum energy, the energy expenditure of placing the second R atom away from the inner ring is still smaller in magnitude than the energy gained from the R–R interaction. Hence, the nuclear configuration of lowest energy for the TR$_2$ complex is that with the two R atoms being located on the same side of the aromatic molecule.

For the TAr$_2$ complex with the first Ar atom located at its original position of minimum energy, the binding energy of the second Ar atom is 1.640 kcal mol^{-1} for the case where the second Ar binds to the same side of the molecule as the first one. If the second Ar atom binds to the opposite side, its binding energy is only 1.534 kcal mol^{-1}. The stabilization energy of the one-sided TAr$_2$ complex relative to the two-faced TAr$_2$ complex is 106 cal mol^{-1} (36 cm^{-1}), which exceeds the zero-point energy of nuclear motion in TAr$_1$. The energy difference between the two isomers

Table V. Binding Energy and Coordinates of the Second Rare-Gas Atom, $R^{(2)}$, in Tetracene-R_2 Complexes[a-c]

	$R^{(1)}$ and $R^{(2)}$ on opposite sides			$R^{(1)}$ and $R^{(2)}$ on same side		
R	y, Å	z, Å	energy, kcal mol⁻¹	y, Å	z, Å	energy, kcal mol⁻¹
Ar	1.10	−3.40	−1.534	−2.75	3.45	−1.640
Kr	1.10	−3.50	−1.825	−2.90	3.55	−1.973
Xe	1.00	−3.70	−2.266	−3.40	3.75	−2.428

[a] With the first atom $R^{(1)}$ frozen at that configuration which corresponds to the potential energy minimum of the TR_1 complex. [b] Coordinates to within ±0.05 Å. $X = 0$. [c] The total energy of the configurations, with both R atoms on the same side, can be lowered if the $R^{(1)}$ position is allowed to vary (the coordinates of $R^{(2)}$ will also change to maintain the optimum R-R distance).
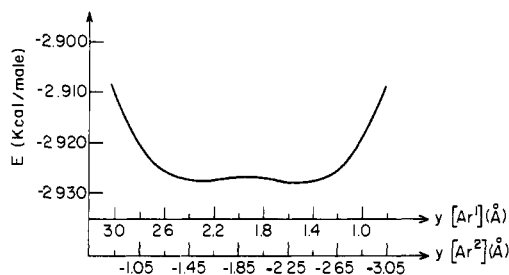

Figure 4. Potential energy (kcal mol⁻¹) as a function of the y coordinate of Ar^1 and Ar^2 for interaction between tetracene and Ar_2. The Ar–Ar distance is fixed at 3.85 Å. $x = 0$ and $z = 3.4$ Å for both Ar_1 and Ar_2.

is sufficiently large to make only the one-sided TAr_2 complex stable. Further refinement of the equilibrium nuclear configuration of the one-sided TAr_2 complex will lead to a further increase in binding energy. However, as we shall subsequently show, this effect is small; so we shall defer the discussion of further nuclear rearrangement until we consider other TR_2 complexes. As is the case of the TAr_2 complex the energetically preferred configuration for TKr_2 and TXe_2 corresponds to that with the second R atom being located on the same side of the molecule as the first. Table V lists the coordinates and binding energies (uncorrected for zero-point motion) for the second R atom calculated for both the one-sided and the two-faced configurations of TR_2 complexes. In all cases, the first R atom was taken to be frozen at the position corresponding to the minimum potential energy of the respective TR_1 complex. For all three noble gases the energy is at least 100 cal mol⁻¹ lower if the two R atoms are located on the same side of the aromatic molecule.

Clearly, the configuration of minimum energy for the TR_2 complex will not be necessarily the one with the first R atom located at its original position of minimum energy. As additional R atoms join the cluster, it is expected that the coordinates of those R atoms already bound to the tetracene will undergo a geometrical reorganization. For the energetically favored one-sided TR_2 molecules we find that this additional geometrical reorganization has a minor effect on the energetics; however, this effect is of considerable intrinsic interest as it provides insight into some features of nuclear dynamics in these dimers. Detailed numerical calculations were performed for the TAr_2 molecule. Figure 4 displays the potential surface for the motion of the Ar–Ar pair along the long y axis of the tetracene molecule. The x and z coordinates were fixed at their optimum lowest energy values, corresponding to $x = 0$ and $z = 3.45$ Å. The Ar–Ar distance was kept constant at its equilibrium configuration of 3.85 Å. Several features of the potential surface for TAr_2 (Figure 4) are of interest. First, the minimum of the potential surface is located at the configuration $y_1 = 1.50$ and $y_2 = -2.40$ Å, where the total energy of TAr_2 (incorporating also the Ar–Ar interaction) is 3.168 kcal mol⁻¹ while, when the first Ar atom is frozen at the TAr_1 equilibrium configuration at $y = 1.10$ Å, the total potential energy of TAr is 3.163 kcal mol⁻¹. Consequently, the lowering of the potential energy of the cluster, due to geometrical reorganization

Table VI. Binding Energies of the Third Rare-Gas Atom for Each of Three Local Minima in the Tetracene-R_3 Complexes

		coordinates and binding energy of the third rare-gas atom			
R	config	x	y	z	energy, kcal mol⁻¹
Ar	A[a]	0.0	3.85	3.45	−1.42[c]
	B[b]	0.0	1.10	−3.40	−1.542
	C[c]	3.25	0.0	3.15	−1.515[d]
Kr	A[a]	0.0	3.9	3.55	−1.644[c]
	B[b]	0.0	1.05	−3.50	−1.838
	C[c]	3.4	0.0	3.20	−1.835[d]
Xe	A[a]	0.0	4.30	3.80	−1.835[c]
	B[b]	0.0	1.00	−3.70	−2.288
	C[c]	3.8	0.0	3.2	−2.327[d]

[a] Bound R_2 displaced so that one rare-gas atom is located at $y = 0$. [b] Bound R_2 in symmetric configuration. [c] Corrected for energy lost from displacement of R_2 pair. [d] Total energy can be slightly lowered if rare-gas atoms are moved in the -x direction.

involving motion along the y axis, is trivially small. Second, the potential surface for the motion of Ar_2 on the surface of tetracene is, strictly speaking, double humped. However, the height of the potential barrier is only 1.5 cal mol⁻¹ (0.5 cm⁻¹), being very small relative to relevant zero-point energies and will not affect the nuclear motion. Third, the potential for the nuclear motion of the Ar_2 dimer can be considered as a shallow potential well. The Ar_2 dimer is expected to undergo a large-amplitude motion with a huge amplitude of ∼1.5 Å along the y axis.

From these calculations of the potential surface of TR_2 complexes, we conclude the following: (1) The one-sided complex is energetically favored. (2) The energy difference between the one-sided TR_2 complex and its two-faced isomer is ∼100 cal mol⁻¹ (35 cm⁻¹), being sufficient to insure the energetic stability of a single structure of TR_2. Thus, no chemical isomers of TR_2 are expected to be exhibited at low temperatures. (3) The nuclear motion of the Ar_2 pair on the surface of tetracene is characterized by a very large amplitude.

TR_3 Complexes. The TR_3 complexes are somewhat more complicated. To simplify the treatment we have assumed that the first two R atoms bind to the same side of the aromatic ring and searched for the energetically favored configurations when the third atom was added. We have considered three plausible structures for the TR_3 complex. (A) *Same-sided collinear*: All three R atoms are placed on one side along the y axis (at $x = 0$). (B) Opposite-sided collinear: An R_2 dimer is located on one side and an R atom is placed on the other side of the ring. (C) Same-sided triangular: Two R atoms are placed along the y axis (at $x = 0$), while the third R atom is located toward the hydrogen atoms (see Figure 5). In our model calculations for TR_3 the distance between the first two R atoms centered on the y axis was kept fixed at the values corresponding to the equilibrium separation in the R_2 dimer, the R_2 pair being placed symmetrically along the y axis, i.e., $y(R_1) - y(R_2)$ and then the third R atom was added. Subsequently, necessary dislocation of the R_2 dimer along the y axis was performed and the (small) energy contribution required to move the R_2 pair was incorporated in the binding energy of the third atom. Finally, the minimum energy and the equilibrium configuration of the third R atom for configurations A, B, and C were determined. The lowest energy structure of the same-side collinear configuration (A) is the symmetric one. Table VI presents the binding energies of the third R atom that is defined as the energy difference between the TR_3 structure and the energy of the equilibrium TR_2 structure. The lowest energy structure for the same-sided collinear configuration (A) is the symmetric one with the coordinates of the central R atom being $y = x = 0$. The energetics of the opposite-sided configuration (B) essentially corresponds to additive effects from binding in TR_2 and TR_1 complexes, the interaction between the R atoms located on opposite sides of the ring being minor. Accordingly, the equilibrium structure of configuration B corresponds to that of TR_2 on one side and that of TR_1 on the other side of the aromatic ring. In
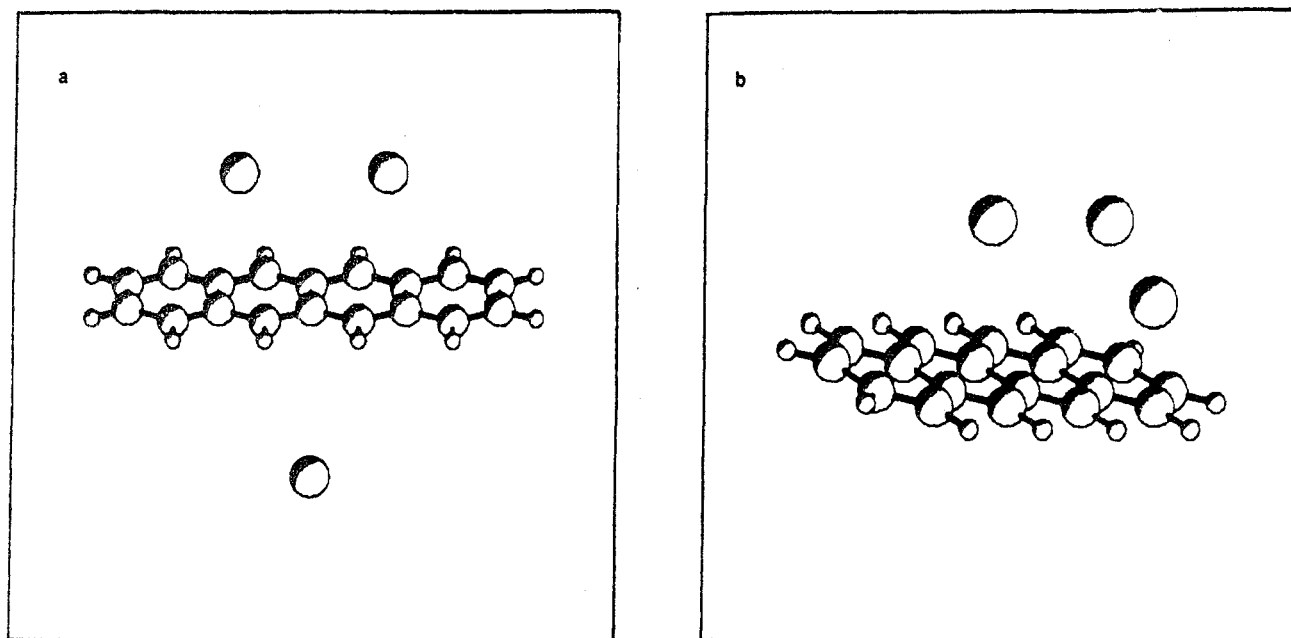
Potential Surfaces of van der Waals Complexes

J. Am. Chem. Soc., Vol. 103, No. 22, 1981 6591

Figure 5. Tetracene–Ar_3. Some possible structures: (a) opposite side; (b) same-sided triangular.

the calculation for the same-sided trigonal configuration (C), R_2 was maintained in the symmetric configuration. The equilibrium configuration of the third R atom, which is moved toward the hydrogen atom, was found to be in the plane bisecting the central bond ($y = 0$) and being somewhat pushed down toward the aromatic ring.

From the model calculations summarized in Table VI, several conclusions emerge concerning the energetic stability of TR_3 molecules. Firstly, the same-sided collinear configuration (A) is always appreciably higher in energy relative to configurations B and C. The stabilization energies of configurations B or C relative to configuration A are ~ 100 cal mol^{-1} for TAr_3, ~ 200 cal mol^{-1} for TKr_3, and ~ 500 cal mol^{-1} for TXe_3. These stabilization energies exceed both the energies of zero-point motion and the low internal temperatures achieved by cooling these complexes in supersonic beams. We thus conclude that the same-sided collinear configuration is energetically unstable. Secondly, the energies of the opposite-sided configuration (B) and the same-sided configuration (C) are very close. The minimum potential energy of configuration B relative to configuration C are -27 cal mol^{-1} (-9 cm^{-1}) for TAr_3, -3 cal mol^{-1} (-1.2 cm^{-1}) for TKr_3. and 39 cal mol^{-1} (14 cm^{-1}) for TXe_3. These stabilization energies should not be taken seriously, as our rough model calculations, which rest on crude potential parameters, cannot provide any reliable information concerning such small energy differences. Our calculations for the TR_3 complexes raise the distinct possibility of peaceful coexistence of two chemical isomers, which will be amenable to experimental observation even at very low temperatures accomplished in supersonic expansions. This pattern of nearly isoenergetic chemical isomers is expected to be exhibited for large TR_n complexes, which are characterized by a high coordination number $n > 3$.

Discussion

Our model calculations of the potential surfaces of vdW complexes, consisting of aromatic molecules and R atoms, are useful for the elucidation of some interesting features of structure, energetics, and nuclear motion of these molecular species. Our admittedly crude calculations of the potential surfaces, which rest on simple recipes for the determination of the potential parameters, should be regarded as the first step in the exploration of the nuclear states of these interesting complexes. Several possible extensions and refinements of the model calculations are possible and practical. The major improvement of the details of the calculations should involve the replacement of the empirical atom–atom potential parameters by direct calculations of the intermolecular

potential between an R atom and an aromatic molecule. This is a formidable task. However, the long-range attractive interactions can be evaluated by the use of a monopole expansion in a manner reminiscent of the treatment of dispersive interactions between two large aromatic molecules developed by Coulson and Davis[31] and Hirschfelder et al.[32] The direct quantum mechanical evaluation of the repulsive interactions between an R atom and an aromatic molecule is much more difficult and one will have to rely on semiempirical methods. We are currently investigating rare-gas aromatic molecule interactions in the ground state and in electronically excited configurations by nonempirical method to gain further insight into the nature of the potential surfaces and for the understanding of the spectral shifts in the electronic spectra of the aromatic molecule induced by the R atoms.

The predictions emerging from our model calculations concerning the energetically favored equilibrium configurations, some of the features of the low-frequency nuclear motion, and the possibility of the existence of several nearly isoenergetic chemical isomers of the TR_n molecule can be confronted with the results of recent spectroscopic studies[22-24] of TR_n molecules ($R = Ne$, Ar, Kr, and Xe) in supersonic expansions. Our model calculations led to the following predictions concerning energetics and structure of the large TR_n molecules.

(1) The binding energies of TR_1 molecules are 530 cm^{-1} for TAr_1, 630 cm^{-1} for TKr_1, and 780 cm^{-1} for TXe_1. Although the exact numerical values should not be taken too seriously, they indicate large bond energies for vdW binding of R atoms to large aromatic molecules. The experimental study[24] of vibrational predissociation of TKr_n molecules led to an upper limit[24] $D_e <$ 1250 cm^{-1} for the binding energy of Kr to T in the first excited singlet state. Correcting this experimental result for the difference in binding energy between the ground and excited state results in an experimental upper limit $D < 1180$ cm^{-1} for binding of a Kr atom to the ground state of T. This experimental upper limit is consistent with the results of our model calculations.

(2) For TR_1 and TR_2 complexes only a single chemical isomer is expected to be energetically stable. This prediction is borne out by the experimental observation[22-24] of a single spectral feature for each of the complexes TAr_1, TAr_2, TKr_1, and TKr_2.

(3) For TR_3 complexes there is a distinct possibility for the existence of two nearly isoenergetic complexes characterized by a two-sided configuration and a same-sided triangular configu-

(31) Coulson, C. A.; Davis, P. L. *Trans. Farad. Soc.* **1952**, *48*, 777.
(32) For example: Hirschfelder, J. O.; Curtiss, C. F.; Bird, R. B. "Molecular Theory of Gases and Liquids"; Wiley: New York. 1954; p 969.

ration. The optical spectrum of the TKr_3 complex shows two separate spectral features,[24] which were tentatively assigned[24] to two distinct chemical isomers and is in accord with the theoretical analysis.

(4) We expect ubiquity of nearly isoenergetic TR_n chemical isomers with high $n > 3$ coordination numbers. The analysis of the TKr_4 spectrum[24] reveals three distinct spectral features, which are due to this complex and which were tentatively assigned[24] to chemical isomers. In general, the spectra of TAr_n, TKr_n, and TXe_n with high $n \geq 4$ values of the coordination number become very complicated.[24] One obvious reason for this spectroscopic complexity is the abundance of chemical isomers.

The appearance of a multiple spectrum with several distinct spectral features, that correspond to a single chemical composition TR_n, does not necessarily originate from the presence of nearly isoenergetic chemical isomers. Our model calculations provide several mechanisms for the occurrence of a multiple spectrum or the intrinsic broadening of spectral features of TR_n complexes with a fixed n. To be more specific let us consider an electronic excitation $S_0 \rightarrow S_1$ of a TR_n complex and focus attention on the 0–0 molecular excitation, where the intramolecular vibrations of T are not excited in the S_1 state. The splitting and broadening of spectral features for the $S_0(0) \rightarrow S_1(0)$ transition of TR_n complexes with a fixed chemical composition can originate from the following causes: (A) Nearly isoenergetic chemical isomers—these were already discussed in this context. (B) Vibrational structure due to T–R intermolecular motion in the S_1 state—in the S_0 electronic state the TR_n molecule is envisioned to be in its vibrationless nuclear state for the T–R intermolecular motion. Vibrational excitations of the T–R motion in S_1 can be excited, provided that (i) the electronic-vibrational transition is symmetry allowed, (ii) the Franck–Condon vibrational overlap is favorable, and (iii) the vibrational frequency is sufficiently high so that the vibrational structure will not be obscured by trivial line broadening (e.g., rotational congestion). Such a vibrational structure will be exhibited toward higher energies from the vibrationless $S_0 \rightarrow S_1$ excitation. Our model calculations indicate that the vibrational frequency for the out-of-plane motion of TR_1 (R = Ar, Kr, and Xe) is in the range 40–50 cm^{-1} and may be amenable to observation. The only evidence for this effect is weak satellite bands in TXe_1 and TXe_2 complexes that are separated from the main spectral feature by 18 cm^{-1} for TXe_1 and 43 cm^{-1} for TXe_2, which were tentatively attributed[24] to the vibrational structure of these complexes. (C) Thermal population of intermolecular T–R vibrational states in S_0—our model calculations demonstrate the existence of low-frequency motion. As a relevant example we consider the large-amplitude nuclear motion in TR_1 and TR_2 complexes along the y molecular axis. The vibrational level spacing for this intermolecular motion is small. Even at the exceedingly low translational, T_t, and rotational, T_r, temperatures ($T_t \sim T_r \sim$ 1–5 K) accessible in supersonic expansions, we expect the thermal population of these low frequency vibrational levels in the S_0 ground electronic state will prevail. As the corresponding frequencies of these low energy intermolecular modes in S_1 are

somewhat different from those in S_0, we expect the appearance of vibrational sequence structure due to the intermolecular motion. This intermolecular vibrational sequence congestion will lead to new spectral features (located either on the red or on the blue side of the vibrationless excitation, depending on the sign of the frequency change) which are very close to the vibrationless transition, so that either congested overlapping spectral features will appear or just unresolved broadening will be exhibited. No definite evidence for this effect is as yet available. (D) The existence of several conformers—when the potential surface of the complex is characterized by two or more close-lying but nondegenerate potential minima, the vibrational structure will consist of several close-lying levels, each corresponding to a distinct conformer. Thermal population of such vibrational states (case C) may result in several distinct vibrational features which correspond to a single complex. The tetracene-R_1 complexes are not expected to exhibit such splitting; however, conformer splitting may be revealed for complexes containing an odd-numbered polyacene, e.g., anthracene-R_1 or pentacene-R_1. Such vibrational conformers qualitatively differ from nearly isoenergetic isomers (case A), as in the latter case the potential barrier separating the two structures is very large.

Our model calculations provide a clue for the understanding of the violation of the additivity law per added R atom (ALPARGA) for the spectral shifts of the TR_n complexes.[29] Levy et al.[5] have observed that for I_2R_n complexes the spectral shift is a linear function of n, obeying the ALPARGA. On the other hand, Amirav et al.[24] have observed the violation of the ALPARGA for TR_n complexes with a deviation of $\sim 30\%$. One way to rationalize the violation of the ALPARGA is to invoke the effects of third-order dispersive interactions. However, it is rather difficult to reconcile the qualitative difference between TR_n and I_2R_n complexes. A reasonable interpretation, which is borne out by our model calculation, is that the R atoms in TR_n complexes occupy geometrically inequivalent sites in complexes with different coordination numbers n, and thus the spectral shifts per R atom induced in TR_n and in TR_{n+1} are expected to be different. We have demonstrated that the equilibrium configuration of each of the two R atoms in TR_2 differ from the position of the single R atom in TR_1, while in TR_3 the third R atom occupies either a one-sided triangular or two-faced configuration, where in both cases the location of the third atom is different from that of the pair of R atoms in TR_2. Although a quantitative treatment of the problem should allow for averaging over the large-amplitude nuclear motion, the general arguments regarding occupation of unequivalent sites remain valid. Consequently, the violation of the ALPARGA is expected, indeed, to be exhibited for the TR_n complexes. On the other hand, in I_2R_n complexes studied by Levy, Wharton, and colleagues,[5] the system is highly symmetric, the R atoms occupying equivalent sites, so that the ALPARGA is obeyed.